

Document downloaded from:

<http://hdl.handle.net/10251/181791>

This paper must be cited as:

Gisbert-Roca, F.; André, FM.; Más Estellés, J.; Monleón Pradas, M.; Mir, LM.; Martínez-Ramos, C. (2021). BDNF-Gene Transfected Schwann Cell-Assisted Axonal Extension and Sprouting on New PLA-PPy Microfiber Substrates. *Macromolecular Bioscience (Online)*. 21(5):1-13. <https://doi.org/10.1002/mabi.202000391>



The final publication is available at

<https://doi.org/10.1002/mabi.202000391>

Copyright John Wiley & Sons

Additional Information

**BDNF-gene transfected Schwann cells-assisted axonal extension and sprouting on new PLA-PPy microfiber substrates**

*Fernando Gisbert Roca, Franck M. André, Jorge Más Estellés, Manuel Monleón Pradas, Lluís M. Mir and Cristina Martínez-Ramos\**

F. Gisbert Roca, Prof. Jorge Más Estellés, Prof. M. Monleón Pradas, Dr. C. Martínez Ramos  
Universitat Politècnica de València  
Centro de Biomateriales e Ingeniería Tisular  
Camino de Vera s/n, 46022, Valencia, Spain  
E-mail: [cris\\_mr\\_1980@hotmail.com](mailto:cris_mr_1980@hotmail.com)

Dr. C. Martínez Ramos  
Universitat Jaume I, Unitat predepartamental de Medicina, Avda/Sos Baynat, S/N, 12071  
Castellón de la Plana, Spain

Prof. M. Monleón Pradas  
CIBER-BBN, Centro de Investigación Biomédica en Red-Bioingeniería, Biomateriales y  
Nanomedicina  
Spain

Dr. Franck M. André, Prof. Lluís M. Mir  
Metabolic and systemic aspects of oncogenesis (METSYS), Université Paris-Saclay, CNRS,  
Institut Gustave Roussy, 94805, Villejuif, France

Keywords: bioengineering, biological applications of polymers, biomaterials, fibers, polypyrroles, conducting polymers, tissue engineering

The work here reported analyses the effect of increased efficiency of brain-derived neurotrophic factor (BDNF) production by electroporated Schwann cells (SCs) on the axonal extension in a co-culture system on a biomaterial platform that can be of interest for the treatment of injuries of the nervous system, both central and peripheral. Rat SCs are electrotransfected with a plasmid coding for the BDNF protein in order to achieve an increased expression and release of this protein into the culture medium of the cells, performing the best balance between the level of transfection and the number of living cells. Gene-transfected SCs show an about 100-fold increase in the release of BDNF into the culture medium, compared to non-electroporated SCs. Co-cultivation of electroporated SCs with rat dorsal root ganglia (DRG) is performed on highly aligned substrates of polylactic acid (PLA) microfibers coated with the electroconductive polymer polypyrrol (PPy). The co-culture of DRG with electrotransfected SCs increase both the axonal extension and the axonal sprouting

from DRG neurons compared to the co-culture of DRG with non-electroporated SCs. Therefore, the use of PLA-PPy highly aligned microfiber substrates pre-seeded with electrotransfected SCs with an increased BDNF secretion is capable of both guiding and accelerating axonal growth.

## 1. Introduction

Injuries produced at the central nervous system (CNS) or at the peripheral nervous system (PNS) are very difficult to treat because they involve cell loss, development of neurotoxic environments and a multiplicity of factors only partially known, which makes spontaneous regenerative processes extremely unlikely<sup>[1,2]</sup>. For this reason, hope for progress towards a greater effectiveness in the regeneration of the nervous system lies in multi-combinatorial solutions that use cell transplantation and biomaterials to guide axonal growth and protect transplanted cells<sup>[3,4]</sup>, as well as the use of different types of stimuli (mechanical, electrical, biochemical) that trigger and accelerate the necessary processes<sup>[5-8]</sup>.

Axonal extension is accompanied and influenced by interactions with auxiliary cells that behave as factories for the biological factors and that play a decisive role in axonal growth<sup>[9,10]</sup>. Schwann cells (SCs) are essential in both the development and the regeneration in the PNS, while oligodendrocytes are essential in the CNS<sup>[11-14]</sup>. SCs are naturally present in the PNS, forming the myelin sheath around the axons and playing a key role in neuronal survival and axonal regeneration<sup>[10,15-17]</sup>. In case of injury, SCs are necessary to achieve the axonal regeneration since they form regeneration columns (called Büngner's bands) that guide the regenerating axons<sup>[11,12]</sup>. SCs also release cytokines such as LIF and IL-6 that promote the survival of neurons<sup>[15]</sup>. In addition, SCs secrete different neurotrophic factors like the nerve growth factor (NGF), brain-derived neurotrophic factor (BDNF) and neurotrophin-3 (NT-3), among others, necessary for axonal regeneration<sup>[15-17]</sup>.

The BDNF protein is present throughout the CNS and is important for the regulation of neuronal survival and differentiation, connectivity, and synaptic plasticity<sup>[18,19]</sup>. BDNF is necessary for the continued survival and phenotypic maintenance of neurons<sup>[19]</sup>, promotes survival of dorsal root ganglion neurons<sup>[20]</sup>, enhances neurogenesis<sup>[20]</sup> and promotes nerve healing and axonal growth, improving axonal regeneration<sup>[21–25]</sup>. The delivery of BDNF *in vivo* to achieve a therapeutic efficacy presents some problems, such as its low stability and short *in vivo* half-life<sup>[19]</sup>. In addition, the use of mini pumps for the delivery of BDNF creates a steep concentration gradient, leading to different problems like the alteration of the infused tissue and different adverse effects such as edemas<sup>[26]</sup>. For these reasons, different techniques can be used to protect the BDNF from the environment and to achieve a controlled and sustained delivery of it without the use of pumps, like the encapsulation of BDNF in biodegradable and biocompatible nano or micro carriers<sup>[27,28]</sup> or the genetic modification of glial cells able to secrete high quantities of this growth factor<sup>[29,30]</sup>, on which this study focuses. In this study, BDNF has been used as a model of neurotrophic factor whose secretion can be increased by genetically modified SCs.

Biological, chemical and physical techniques can be employed to achieve the genetic modification of cells<sup>[31]</sup>. Biological, virus-mediated, transfection is the most used technique in clinical research, since it is highly efficient and it easily achieves a stable transfection<sup>[31,32]</sup>. With this technique, the foreign DNA is integrated into the genome of the cell and it replicates as the host genome does, enabling a sustainable transgene expression<sup>[33,34]</sup>. However, it has been reported that viral vectors integrate into the host genome randomly, which may disrupt tumour suppressor genes, activate oncogenes, or interrupt essential genes, leading to a malignant transformation<sup>[31,35,36]</sup>. For these reasons, non-viral transfection techniques such as electroporation have been widely applied<sup>[31,37]</sup>.

The transfection of SCs to achieve a greater expression and release of BDNF has been previously studied using retroviral vectors, observing an increase in the secretion of BDNF by

infected cells which is between 4.6 and 26 times higher than the BDNF release of non-transfected SCs [29,30]. SCs transfection using electroporation techniques to achieve an increased BDNF secretion *in vitro* or *in vivo* has not been previously studied. Electroporation is a physical technique that offers a safe and fast alternative to achieve the introduction of the plasmid of interest into the target cells and to transiently express the protein that it encodes<sup>[31,37,38]</sup>. If appropriate parameters are determined and used, the electric pulses have exclusively reversible effects (the transient rupture of the membrane impermeability) with no addition of foreign substances. This makes a very important difference with respect to the non-viral transfection techniques based on the chemical vectorization of the nucleic acids, particularly in the case of delicate cells. Indeed, these methods provoke the penetration in the cells or in the cell's membrane of the foreign molecules that transport the nucleic acid, such as liposomal cationic lipids, block-copolymers, etc. or of large supra-molecular complexes such as many types of nanoparticles, organic or inorganic. These residues of the transfection technology may have longer effects than the consequences of the physical approaches such as electroporation, particularly if electric pulses are well tuned to the target cells. Moreover, when electroporation is used, there is no plasmid integration<sup>[31,37]</sup>, which fits with the purposes of the work reported in this manuscript. In our case, a transient transfection of SCs to obtain an increased secretion of BDNF by these cells should be sufficient since the transient expression will last for enough time to carry out the *in vitro* studies. It will also allow future *in vivo* applications with short term, controlled and sustained release of BDNF by SCs. The same approach with little modifications (such as the adjustment of the electric pulses parameters depending on the size of the plasmid) can be foreseen in future studies to achieve increased secretion by the SCs of other neurotrophic factors such as NGF or NT-3.

In order to study the axonal growth, dorsal root ganglia (DRG) are interesting as neuron source because they provide projecting neurons with somata that remain in place while the axon extends. Furthermore, they also contain other auxiliary cells that migrate from the DRG

body (mostly SCs) and generate a cellular environment that favours axonal growth and survival<sup>[39,40]</sup>. Finally, the DRG body edge can be taken as the starting point for the axon's growth, facilitating a reference for the measurement of axonal extension.

Biomaterials interact with cells essentially topographically, through adhesion and mechanotransduction signals<sup>[41,42]</sup>, and they can direct axonal growth towards a target through the mechanical constriction of cells<sup>[43,44]</sup>. However, biomaterials cannot supply the multitude of growth factors and biochemical signals that are necessary for axonal growth and regeneration<sup>[45-48]</sup>. It is essential to understand the behaviour of cells that adhere to the biomaterial, and to check if their trophic factors secretory capacity remains unchanged. The planned strategy was to develop a methodology to enhance this secretory role of SCs, and to check its effect on the extension of axons from DRG neurons over growth-guiding biomaterials.

In previous studies we have developed highly aligned substrates based on the use of polylactic acid (PLA) nano and micro fibers covered with different amounts of the conductive polymer polypyrrole (PPy)<sup>[49,50]</sup>. After performing a scanning of different reaction parameters, the physicochemical and dielectric properties of the substrates were characterized. As a result, the substrates with the least amount of PPy that allowed to obtain a homogeneous coating of the PLA fibers was chosen to carry out the *in vitro* studies with cells. PLA was used as host polymer of the substrates since it is a low cost, renewable, environmentally friendly and biodegradable biomaterial<sup>[51,52]</sup>. Furthermore, its biocompatibility is critical in order to use PLA-PPy substrates for tissue engineering applications<sup>[53,54]</sup>. In addition, the coating of the PLA microfibers with PPy via *in situ* polymerization seemed a good approach, since PPy is an intractable and brittle solid with poor mechanical processability<sup>[55]</sup>. With this strategy we can exploit both the intrinsic electrical conductivity of PPy and the better mechanical properties of the insulating host polymer<sup>[55-57]</sup>.

It is important to note that PPy is an interesting electroconductive material due to its high electrical conductivity, long-term ambient stability, good biocompatibility, low cost and facile synthesis by chemical polymerization<sup>[55,58–61]</sup>. Furthermore, PPy has been commonly used in biomedical applications, especially in nerve tissue engineering scaffolds, due to its good biocompatibility and high electrical conductivity<sup>[56,62–64]</sup>.

Electrically conductive substrates based on intrinsically conductive polymers have been extensively studied in order to improve the axonal extension of neurons and induce a greater release of neurotrophins by glial cells when subjected to an exogenous electric field<sup>[65–67]</sup>. Among all electroconductive polymers, there are well-studied ones like PPy, polyaniline (PANI) and poly(3,4-ethylenedioxythiophene) (PEDOT). Herein, we sought to use PLA - PPy electroconductive highly aligned substrates based on microfibers since we have previously observed that they offer an enhanced axonal guidance and growth versus flat, non-aligned, or smaller fiber sized substrates<sup>[49]</sup>. In addition, the use of electroconductive substrates offers the possibility of its electrically stimulation in future experiments.

Regarding the topography of the substrates, we focus on the use of aligned substrates because they induce a high axonal orientation, whereas in a flat substrate such as a glass cover or a substrate with randomly oriented fibers, axons grow unoriented<sup>[43,44,56,68–70]</sup>. In addition, the diameter of the fibers that form the substrate is an important parameter since it influences the neurite outgrowth and the SCs migration from DRG<sup>[39,40,71]</sup>. We have previously studied different fiber diameters, concluding that micrometer sized fibers (10  $\mu\text{m}$  diameter) provide the best axonal growth<sup>[49]</sup>. Here, we have grouped in parallel 10  $\mu\text{m}$  diameter microfibers with polycaprolactone (PCL) bands that act as fasteners in the extremes to obtain rail shaped microfiber bundles. PCL was used as fastening material for the microfibers bundles due to its low melting point (around 60°C), making possible the fabrication of the microfiber bundles. PCL is a biodegradable and biocompatible polymer that has been commonly used for biomedical applications as an implantable biomaterial<sup>[72,73]</sup>.

In this study, we develop a bioactive device based on the combination of a biocompatible substrate formed by highly aligned electroconductive microfibers (PLA/PPy) and genetically modified SCs with the aim of accelerating the repair of lesions both in the CNS and in the PNS. The highly aligned topography can guide axonal growth to maximize the linear distance that regenerating axons cover, and the use of genetically modified support cells can increase their secretion of growth factors, allowing to increase and accelerate the axonal growth of the neurons seeded on the device. In the frame of optimized biological conditions using rat DRG co-cultured or not with genetically modified rat SCs, we evaluated the new highly aligned microfiber-based substrates, hoping to reach a large axonal sprouting and a sustained and directional axonal growth along these substrates. In addition, the device has electroconductive characteristics, so it is susceptible to electrical excitation and to transmit this type of stimuli.

## **2. Experimental section**

### **2.1. Electroporation of rat Schwann cells**

The plasmid pCMV-GFP (3,487 bp) containing the GFP reporter gene under the cytomegalovirus (CMV) promoter was produced by PlasmidFactory (Bielefeld, Germany) and stored at  $-20^{\circ}\text{C}$  at a concentration of  $1\ \mu\text{g plasmid}/\mu\text{l}$  of Milli-Q<sup>®</sup> ultrapure water. The gene transfection of rat Schwann cells (SCs; P10301, Innoprot) in passage 5 using the pCMV-GFP plasmid was carried out with the BIORAD gene pulser (Gene Pulser Xcell Electroporation System, BIORAD) applying 8 square pulses with a duration of  $100\ \mu\text{s}/\text{pulse}$  and a frequency of 1 Hz in a  $100\ \mu\text{l}$  total volume cuvette with 1 mm between electrodes. The time between the electroporation and the dilution of the cells in culture medium and their introduction into the incubator was 15 min. Apart from these parameters which were kept constant, we varied the other parameters: number of cells; amplitude of the applied voltage (thus of the electric field); volume of Spinner Minimum Essential Medium (SMEM, Thermo



Fisher Scientific); volume of Milli-Q<sup>®</sup> ultrapure water and mass (thus amount) of plasmid. As indicated in Table 1, two controls with a different number of cells (C1 - C2) and seven different electroporation protocols (P1 – P7) were studied in order to determine the best conditions for the electrotransfection of the Schwann cells, based on our previous experience on other cell types<sup>[74,75]</sup>. The goal of these experiments was to produce the maximum amount of transfected living cells which is a trade between the level of electroporation/transfection and the number of cells remaining alive. A detailed explanation of the results obtained for each protocol is described in section 3.1.

Once the best electroporation parameters were obtained using the pCMV-GFP plasmid (protocol P7), it was applied again to rat SCs in passage 5 using the BDNF-SEP plasmid<sup>[76]</sup> which was a gift from Ryohei Yasuda (Addgene plasmid # 83955 ; <http://n2t.net/addgene:83955> ; RRID:Addgene\_83955). We purified this plasmid from Escherichia coli-transformed cells using the NucleoBond PC2000 EF kit (Macherey-Nagel, Hoerd, France) and then we diluted it in Milli-Q<sup>®</sup> ultrapure water. Light absorption at 260 nm was used to determine DNA concentration and the quality of the plasmid was assessed by calculating the ratios of light absorption at 260/280 nm and 260/230 nm. It was stored at a concentration of 4.3 µg plasmid/µl Milli-Q<sup>®</sup> ultrapure water.

After the electroporation of SCs, control and gene-transfected SCs were diluted in normal Schwann cell culture medium and introduced in an incubator at 37°C with a humid atmosphere containing 5% CO<sub>2</sub>. All the cells from a single electroporation cuvette were introduced in a single T25 culture flask.

## **2.2. Quantification of pCMV-GFP plasmid transfection results**

SCs transfected with the pCMV-GFP plasmid were analyzed at different times: after 1, 4, 6 and 11 days of cell culture. Firstly, cells were observed using an inverse microscope (Axio Observer Z1, Carl Zeiss Microscopy) to appreciate the green fluorescence of transfected cells.

Then, after removing the culture medium and thus the dead cells, culture flasks were washed with PBS and a trypsin/EDTA solution (T/E; 25200-072, Life Technologies) was then added to break the cell-matrix and cell-cell interactions in order to remove the cells from the bottom of the culture flask. After centrifugation at 1,080 rpm for 5 min, the pellet was resuspended in Schwann cell culture medium (P60123, Innoprot) and the total number of cells was counted. Half of the cells in suspension were re-seeded in a T25 flask and the rest were analysed by flow cytometry (10,000 events were recorded) using the green fluorescence channel (excitation 488 nm, emission 530 nm) in a C6 Accuri flow cytometer (BD, San José, California, USA). As a result, the number of living cells (total number of cells), the level of transfection (percentage of cells showing green fluorescence) and the number of transfected living cells (multiplication of the two previous parameters) were collected.

### **2.3. Preparation of PLA-PPy microfiber bundles**

Highly aligned PLA microfiber (MF) bundles were manufactured by grouping 1,200 PLA MFs with a diameter of 10  $\mu\text{m}$  (Aitex, Spain). PCL bands that acted as fasteners were used at the extremes of the MFs to maintain the alignment and the lane-shaped disposition. PCL bands were placed in a solid state on both extremes of the bundle and melted so, once cooled, the MFs were attached by the PCL bands. MF substrates with dimensions of 17 mm x 3 mm (length x width) were used. The auxiliary PCL bands that maintain the MF together are not considered when defining the dimensions of the MF substrates.

MF substrates were coated with the electrically conductive polymer PPy via *in situ* polymerization. Firstly, the substrates were immersed in deionized water and a fixed vacuum was applied until the substrates stopped floating. With this procedure the introduction of water inside the spaces between fibers was achieved to obtain a homogeneous coating of all MFs, not only the superficial ones. Next, each substrate was introduced into a polypropylene tube with an aqueous solution of pyrrole monomer (Py, Sigma-Aldrich 131709) and sodium

para-toluene sulfonate (pTS, Sigma-Aldrich, 152536) that acted as dopant. It was followed by ultrasonication for 1 min to allow the membrane to be saturated with Py/pTS aqueous solution. The substrates were incubated with shaking at 4°C for 1 h. The ratio between the substrates area (length x width) and the final volume of the Py/pTS aqueous solution was 0.6 cm<sup>2</sup>/ml and a concentration of 14 mM was used for both Py and pTS. Then, an aqueous solution of ferric chloride (FeCl<sub>3</sub>, Sigma-Aldrich 157740) that acted as oxidant was added and incubated with shaking at 4°C for 24 h for the polymerization and deposition of PPy on the PLA substrates. The ratio between the substrates area (length x width) and the final volume of the FeCl<sub>3</sub> aqueous solution was 0.6 cm<sup>2</sup>/ml and a concentration of 38 mM of FeCl<sub>3</sub> was used. PPy-coated membranes were washed with deionized water with agitation for 10 min for three times and ultrasonicated for 30 min in deionized water for three times. Finally, the membranes were dried in a desiccator with a fixed vacuum at 40°C for 2 days.

#### **2.4. Morphological characterization by field emission scanning electron microscopy (FESEM)**

In order to characterize the surface morphology of PLA-PPy substrates a field emission scanning electron microscope (FESEM; ULTRA 55, ZEISS Oxford Instruments) was employed. During the 24 h prior to the test the samples were desiccated under vacuum conditions to avoid interferences caused by evaporated water. After that, samples were placed on the top of a carbon tape creating a carbon bridge between the samples and the carbon tape and they were coated with a thin layer of platinum. Finally, the images were taken applying a voltage of 2 kV.

#### **2.5. Substrates sanitization and preconditioning**

To sanitize the PLA-PPy MF substrates prior to the cell culture, they were immersed in 70% ethanol (ET00021000, Scharlab) for 3 washes of 10 min. Following, 4 washes of 10 min with sterile Milli-Q<sup>®</sup> ultrapure water were applied to remove the ethanol residues.

Finally, the substrates were preconditioned by immersion in Dulbecco's Modified Eagle Medium with a high glucose level (4.5 g/L) (21331020, Life Technologies) supplemented with 10% Fetal Bovine Serum (10270-106/A3381E, Life Technologies), Penicillin (100 U/mL) and Streptomycin (0.1 mg/mL) (Penicillin/Streptomycin, 15140122, Life Technologies) and incubation at 37°C for 24 h in a humidified atmosphere containing 5% CO<sub>2</sub>.

### **2.6. Schwann cells culture on PLA-PPy substrates**

The culture of rat Schwann cells (SCs) in passage 5 and BDNF-SEP transfected SCs (eSCs) 24 h after electroporation was performed on PLA-PPy MF substrates (n=12 per group) during 24 h in order to allow the cells to attach to the substrates before the DRG seeding.

Firstly, the culture medium was removed in order to discard dead cells. Next, the cell culture flasks containing the cells were washed with PBS and then a trypsin/EDTA solution (T/E; 25200-072, Life Technologies) was incorporated to break the cell-matrix and cell-cell interactions with the objective of detach cells from the bottom of the flasks. Finally, a centrifugation at 1080 rpm for 5 min was applied and the pellet was resuspended in Schwann cell culture medium (P60123, Innoprot). After counting the number of cells present, SCs and eSCs were seeded with a seeding density of 100,000 cells per substrate through the deposit of 2 drops of 5 µl (50,000 SCs per drop) at equidistant points from the substrate extremities to spread the cells along the substrate, specially at its extremes (**Figure 1**). Each substrate was placed in a different well of a P12 well plate (Nunc A/s, Roskilde, Denmark) containing 1 ml of Schwann cell culture medium. Finally, the samples were introduced in an incubator at 37°C with a humid atmosphere containing 5% CO<sub>2</sub> for 24 h, until the next day in which the DRG were seeded.

### **2.7. Dorsal root ganglions culture on PLA-PPy substrates**

Dorsal root ganglia (DRG) from 5 days old Wistar rats were extracted and seeded on the centre of PLA-PPy substrates (Figure 1). Three different groups were studied (n=12 per group): DRG seeded on substrates without pre-seeded SCs (DRG), DRG seeded on substrates pre-seeded with SCs (SCs + DRG) and DRG seeded on substrates pre-seeded with BDNF-SEP transfected SCs (eSCs + DRG). Each substrate was placed in a different well of a P12 well plate containing 3 ml of neurobasal culture medium (21103-049, Thermo Fisher Scientific) with 2% D-(+)-Glucose 0.56 M (G8644, Sigma-Aldrich), 0.25% L-Glutamine 200 mM (25030024, Thermo Fisher Scientific), Penicillin (100 U/mL) and Streptomycin (0.1 mg/mL) and 1% Fetal Bovine Serum (10270-106/A3381E, Life Technologies). Finally, the samples were introduced in an incubator at 37°C with a humid atmosphere containing 5% CO<sub>2</sub> for 5 days to study the axonal growth and axonal extension.

### **2.8. Quantification of BDNF secretion**

The quantity of BDNF present in the cell culture supernatant of the three studied groups (DRG, SCs + DRG and eSCs + DRG) was quantified after 1, 2 and 5 days of cell culture. For it, 100 µl of culture medium were removed from every well at each time and the total BDNF Quantikine ELISA Kit (DBNT00, R&D Systems) was employed (n=3) for the quantification. A standard curve was performed to convert the obtained absorbance into BDNF concentration.

### **2.9. Immunostaining of SCs and DRG**

After culture, cells were fixed with 4% paraformaldehyde (PFA; 47608, Sigma-Aldrich) for 20 min at room temperature. Then, 3 washes of 10 min with PB 0.1M were carried out and the cell membrane was permeabilized by the use of a blocking buffer composed of PB 0.1M with 3% bovine serum albumin (BSA; A7906, Sigma-Aldrich) and 0.1% Tween-20 (P1379, Sigma-Aldrich) for 1 h at room temperature.

SCs were stained with rabbit monoclonal anti-S100 beta antibody (ab52642, abcam, 1/200 dilution) and neurons were stained with mouse monoclonal anti-beta III tubulin antibody

(ab7751, abcam, 1/500 dilution), and then incubated at 4°C overnight. Secondary antibodies, goat anti-rabbit IgG Alexa Fluor® 555 (A-21429, Thermo Fisher Scientific, 1/200 dilution) and goat anti-mouse IgG Alexa Fluor® 488 (A-11029, Thermo Fisher Scientific, 1/200 dilution), were used for another 2 hours at room temperature in the darkness. Afterwards, samples were incubated with DAPI (D9564, Sigma-Aldrich, 1/1000 dilution) for 10 min to mark the cells' nuclei. The imaging was performed employing an inverse microscope (Axio Observer Z1, Carl Zeiss Microscopy).

### **2.10. Quantification of axonal extension, axonal sprouting and SCs coverage**

The methodology followed for the quantification of axonal extension and axonal sprouting is explained in detail in<sup>[49]</sup>. Below we proceed to explain it briefly.

Using the ImageJ/FIJI image processing software<sup>[77]</sup> both the maximum length and the area of axons were measured. On the one hand, the maximum length of axons was considered as the distance between the edge of the DRG body and the end of the longest axon (studying both the maximum of both sides and the sum of both sides). On the other hand, the area of the axons was calculated by subtracting the area of the DRG body from the total area of the DRG. In addition, the axonal sprouting was quantified by analysing the DRG images using an in-house software developed under MATLAB R2018a (The MathWorks, Inc.). The centre and the left and right edges of the DRG body were obtained as the maximum point of the relative intensity and as the maximum and minimum values of the relative intensity gradient, respectively. Then, three different parameters were obtained: the distance covered by the Sprouts between the point that corresponds to the centre of the DRG body ( $I_{\text{centre}}$ ) and the point where  $I_{\text{centre}}$  is reduced by 75% ( $S_{\text{centre}}$ , Equation 1), the distance covered by the Sprouts between the point that corresponds to the edge of the DRG ( $I_{\text{edge}}$ ) and the point where  $I_{\text{edge}}$  is reduced by 75% ( $S_{\text{edge}}$ , Equation 2) and the area under the curve (AUC) between the point that corresponds to the edge of the DRG body ( $I_{\text{edge}}$ ) and the point where  $I_{\text{centre}}$  is reduced by 80%

( $S_{AUC}$ , Equation 3). All the parameters were obtained for both sides of the DRG body and the sum of both values was considered.

$$S_{centre} = Distance \left( I_{centre}, \frac{I_{centre}}{4} \right) \quad (1)$$

$$S_{edge} = Distance \left( I_{edge}, \frac{I_{edge}}{4} \right) \quad (2)$$

$$S_{AUC} = Area \left( I_{edge}, \frac{I_{centre}}{5} \right) \quad (3)$$

In addition, the length and the area of the SCs coverage formed on the substrate were quantified. These parameters were obtained for both sides of the DRG body and the mean of both values was considered.

### 2.11. Quantification of axonal alignment

In order to characterize the alignment of axon bundles in the direction of PLA-PPy microfibers, we compared the angle of the microfibers with the angle of the axon bundles that were present over each specific microfiber (using the ImageJ/FIJI image processing software). After measuring the angle of a microfiber and the angle of the axon bundle that was present over that specific microfiber, the difference between both values was obtained in absolute value (**Figure S1**). The process was repeated for several different microfibers in each sample (n=6) and the mean of those values was obtained. Finally, the mean value for all the samples in each studied group (DRG, SCs+DRG and eSCs+DRG) was obtained. In this procedure only axon bundles that follow the direction of the microfibers are considered, discarding the axon bundles that occasionally cross or jump from one fiber to another.

### 2.12. Statistical analysis

Results are expressed as mean  $\pm$  standard error of the mean (SEM). The statistical analysis of the results was performed with GraphPad Prism® software using the one-way ANOVA test together with a multiple sample mean comparison (Tuckey's multiple comparisons test with a

significance degree of 95%) in order to reveal significant differences between conditions. Statistically significant differences are indicated by \*, \*\*, \*\*\* or \*\*\*\*, indicating a p-value below 0.05, 0.01, 0.001 or 0.0001, respectively.

### 3. Results and discussion

#### 3.1. Optimization of electroporation parameters of Schwann cells using the pCMV-GFP plasmid

In order to obtain the electroporation parameters that provide the maximum number of transfected living cells, a scan of the electroporation conditions that were considered more critical (applied electric field, amount of plasmid, amount of water and number of cells) was carried out based on our previous experience<sup>[74,75]</sup>. The rest of parameters (number, shape, duration and frequency of pulses and time between the electric pulses delivery and the dilution and introduction of the cells in the incubator) remained unmodified. Cuvettes with a volume of 100  $\mu$ l and a gap between electrodes of 1 mm were used to apply the highest electric field amplitudes with small currents.

**Table 1.** Detail of the variable parameters of the 2 control conditions and the 7 protocols explored.

	C1	C2	P1	P2	P3	P4	P5	P6	P7
Number of cells	$5 \cdot 10^5$	$1 \cdot 10^6$	$5 \cdot 10^5$	$5 \cdot 10^5$	$5 \cdot 10^5$	$5 \cdot 10^5$	$5 \cdot 10^5$	$5 \cdot 10^5$	$1 \cdot 10^6$
SMEM (% v/v) / Water (% v/v)	100/0	100/0	96/4	44/56	44/56	44/56	44/56	25/75	44/56
Plasmid mass ( $\mu$ g)	0	0	4.5	4.5	4.5	50	50	50	50
Electric field amplitude (V/cm)	0	0	1,000	1,000	1,500	1,500	2,000	2,000	2,000

P1, P2 and P3 protocols were performed to know the effect of the amount of water and the applied electric field in the case of low quantities of cells and plasmid. On the one hand, it was observed (**Figure 2**) that increasing from 4% to 56% the volume percentage of water (P1



vs P2) considerably improved both the level of transfection and the number of transfected living cells, thanks to increasing the difference in concentrations between the inside and the outside of cells. On the other hand, according to Figure 2, increasing the applied electric field from 1,000 V to 1,500 V (P2 vs P3), keeping the volume percentage of water at 56%, further improved the level of transfection and the number of transfected living cells.

With the P4 protocol the effect of increasing the amount of plasmid was studied, increasing the plasmid mass from 4.5  $\mu\text{g}$  to 50  $\mu\text{g}$  (P3 vs P4). As can be seen in Figure 2, it increased the level of transfection, but the higher cell death led to obtain a quantity of transfected living cells similar to that obtained with the P3 protocol.

To study the effect of increasing the applied electric field from 1,500 V to 2,000 V (P4 vs P5) protocol P5 was carried out. As it can be observed in Figure 2, an increase of the level of transfection was obtained with a low increase of cell death, resulting in the increase of the transfected living cells. Therefore, SCs are able to tolerate this applied electric field quite well.

With the P6 protocol, the volume percentage of water was increased from 56% to 75% (P5 vs P6). According to Figure 2, the higher water content slightly improved the level of transfection, but the higher level of cell death caused a considerable decrease in the number of transfected living cells. Consequently, SCs cannot tolerate this high quantity of water in the cell culture medium.

Since the objective was to achieve the largest number of transfected living cells, the P5 protocol was modified and the number of cells present in the electroporation cuvette was doubled from 500,000 to 1 million cells (protocol P7). The P7 protocol derives from the P5 protocol because the latter provided already a high level of transfection and the highest number of transfected living cells when 500,000 cells were used. As a result, a level of transfection slightly higher to the one obtained with P5 protocol was obtained, with a quite low cell death, using the same amount of DNA. This, together with the higher number of cells that were used, led to a very high number of transfected living cells, doubling the results

obtained with P5 protocol. Therefore, the P7 protocol was chosen to carry out the electroporation of SCs with the BDNF-SEP plasmid (section 3.2), since it provided the largest number of transfected living cells per cuvette and per  $\mu\text{g}$  of DNA. As it can be observed in Figure 2, the survival of the SCs transfected using the P7 protocol is very high, similar to the survival in the C2 control group, at least for 11 days. In addition, the images of fluorescence microscopy reveal not only the level of transfection, but also that the transfected SCs survive well and display a healthy morphology.

### **3.2. Quantification of secreted BDNF by Schwann cells transfected with the BDNF-SEP plasmid**

Using the P7 electroporation protocol (Table 1), SCs in passage 5 were transfected with the BDNF-SEP plasmid. Next, SCs and eSCs (24 hours after electroporation) were seeded on PLA-PPy MF substrates (**Figure 3**) by 2 equidistant drops of 5  $\mu\text{l}$  (50,000 SCs per drop) to spread the cells along the substrate, specially at its extremes. As can be observed in Figure 3, PLA-PPy microfibers have a high alignment thanks to the PCL bands that act as fasteners at its extremes. In addition, there is a homogeneous coating with PPy in the form of fine grain texture that can be seen in the whole surface, with just some loose aggregates that mostly disappear with repeated washing. The physico-chemical and electrical properties of the PLA-PPy substrates employed in this study have been extensively characterized in previous papers.<sup>[49,50]</sup> The presence of the PPy coating was confirmed by Fourier-Transform Infrared Spectroscopy (FTIR), observing the characteristic peaks of PLA, PPy, and pTS.<sup>[50]</sup> The mass fraction of PPy ( $3.5 \pm 0.7 \%$ ) and the thickness of the PPy coating ( $122 \pm 8 \text{ nm}$ ) were also quantified.<sup>[49]</sup> Regarding the electrical characterization, a conductivity of  $1.36 \pm 0.08 \text{ S/cm}$  was obtained for the PLA-PPy substrates used in this study.<sup>[49]</sup> The distribution and the morphology of pre-cultured SCs and DRG on PLA-PPy substrates were also studied.<sup>[49]</sup> Regarding the SCs, no significant effect of the PPy coating was observed on the distribution, motility, or morphology of these cells.<sup>[49]</sup> For the DRG, the PPy coating resulted in an

additional promoting effect on axonal growth, possibly produced by the greater surface roughness of the PPy-coated substrates that favors the adhesion of the DRG.<sup>[49]</sup>

To allow cell adhesion, SCs and eSCs were cultured on PLA-PPy substrates for 24 hours. Then, DRG were seeded in the middle of three different substrates (one DRG per substrate): substrates without precultured cells (DRG), substrates with a previous culture of SCs during 24 h (SCs + DRG) and substrates with a previous culture of eSCs during 24 h (eSCs + DRG). One, two and five days after the DRG seeding, the quantity of BDNF present in the cell culture supernatant was measured by ELISA. As it can be observed in **Figure 4A**, when DRG are seed alone without precultured SCs (DRG) there is a weak liberation of BDNF from SCs that migrate from the DRG body. However, when DRG are seeded in substrates with precultured SCs (SCs + DRG) there is an increase of the secreted BDNF due to the higher amount of SCs that are present (precultured SCs and SCs that come from the DRG). This corroborates that SCs secrete naturally the BDNF protein, but at low quantities.

Regarding the group with a previous culture of eSCs (eSCs + DRG) the secretion of BDNF to the culture medium greatly increases (Figure 4B). As it can be observed, when genetically unmodified SCs are used, the quantity of BDNF present in the medium after 5 days of cell culture is around 8 pg/ml, while when eSCs are used the quantity of BDNF increases to around 800 pg/ml (100 times more). With this result we can confirm that the BDNF-SEP plasmid has been correctly taken up by almost of the cells and that the transcription machinery of SCs is able to express the BDNF protein. In addition, the SCs are able to naturally secrete this excess of BDNF protein into the culture medium, secreting much more BDNF than non-electroporated SCs.

In order to check the presence of precultured SCs and eSCs, fluorescent images ( $\beta$  III Tubulin, DAPI and S 100  $\beta$ ) of samples after 5 days of DRG culture were studied (**Figure 5**). Firstly, a global image of each sample is presented for each group (A-C for the DRG group, D-F for the SCs + DRG group and G-I for the eSCs + DRG group). Secondly, two different zones are

presented for each sample: one at the end of the axons (A1-C1 for the DRG group, D1-F1 for the SCs + DRG group and G1-I1 for the eSCs + DRG group) and another far away from the axons (A2-C2 for the DRG group, D2-F2 for the SCs + DRG group and G2-I2 for the eSCs + DRG group).

For the DRG group the SCs are only present very near to the axons, with no SC in areas where axons are not present (Figure 5A-C). This indicates that axons grow together with SCs that migrate from the DRG body, and therefore, the presence of SCs is a necessary requirement for axonal growth. However, for the SCs + DRG (Figure 5D-F) and eSCs + DRG (Figure 5G-I) groups, SCs are present far away from the axons, indicating that these cells are the pre-seeded ones, and not SCs that come from the DRG body. In order to confirm this presence of the pre-seeded SCs (both unmodified and genetically transfected) we measured the length and the area of the SCs coverage present on the substrate after 5 days of DRG culture (**Figure 6**). Both the length and the area of the SCs coverage are clearly larger for the groups with pre-seeded SCs (SCs + DRG and eSCs + DRG), confirming the presence of the pre-seeded SCs. Furthermore, there is no statistically significant difference in the length or in the area covered by the SCs between the SCs + DRG and eSCs + DRG groups, which is indicative of the good survival of the eSCs.

In addition, there is a great increment of axonal growth when precultured eSCs are used (eSCs + DRG group) when compared with the DRG cultured without precultured SCs (DRG group) (Figure 5). For the DRG + SCs group there is an intermediate behaviour. This indicates that the precultured SCs are able to support the axons, increasing the axonal growth rate. In addition, the increased secretion of BDNF by eSCs to the culture medium increases even more the axonal growth rate. A quantification of axonal extension and sprouting for the three groups is done in section 3.3.

### **3.3. Quantification of axonal extension and axonal sprouting on PLA-PPy substrates**

In order to quantify the axonal growth on the three different groups (DRG, SCs + DRG and eSCs + DRG), both the axonal extension and the axonal sprouting were quantified. It is important to study these two characteristics because the axonal extension refers to the maximum length that axons can reach, and the axonal sprouting refers to the quantity of axons that are emerging from the DRG body. To do so, six different parameters were measured from fluorescent microscope images ( $\beta$  III Tubulin) of samples after 5 days of DRG culture. On the one hand, the maximum length of axons (maximum and sum of both sides) and the area of axons were obtained to quantify the axonal extension. On the other hand, the parameters  $S_{\text{centre}}$ ,  $S_{\text{edge}}$  and  $S_{\text{AUC}}$  were obtained to study the axonal sprouting. As it can be observed in Figure 5, the high alignment of PLA-PPy substrates results in a high directionality of axons in the direction of the fibers, maximizing the lineal distance that axons travel. This high directionality was quantified by measuring the angular difference between the direction of axon bundles and the direction of microfibers, obtaining a very low difference between both directions:  $1.4 \pm 0.2^\circ$ ,  $1.5 \pm 0.2^\circ$ , and  $1.2 \pm 0.1^\circ$  for the DRG, SCs + DRG and eSCs + DRG groups, respectively.

As it can be observed in **Figure 7**, the presence of precultured SCs is critical in order to increase the axonal extension, since the maximum length of axons (sum of both sides) displays a 91.8% increase and the area of axons a 126.2% increase when the SCs are present. According to Figure 5, when DRG are seeded alone without precultured SCs, the axons arrive as far as the SCs that migrate from the DRG body. This proves that axons do not grow without the direct support of SCs and so their growth rate depends directly on the migration rate of SCs from the DRG body. However, when precultured SCs are present in areas far away from the DRG body, axons are able to increase their growth rate thanks to the support of the precultured SC cells, since axons do not have to wait for SCs from the DRG. The effect of precultured SCs is also noticeable for axonal sprouting, since an increase in  $S_{\text{centre}}$ ,  $S_{\text{edge}}$  and  $S_{\text{AUC}}$  of 57.1%, 25.8% and 68.3%, respectively, is observed when precultured SCs are present.

This indicates an effect of precultured SCs that are near the DRG body, so the axons do not need to wait for the SCs migration from the DRG body and can start to grow earlier.

Regarding the effects of eSCs, we observe that, in addition to the effect observed when non-electroporated SCs are used, the higher concentration of BDNF that is present in the cell culture medium when eSCs are used is able to further increase the axonal growth, observing an increase of both axonal extension and axonal sprouting. For the eSCs + DRG group, an increase of 34.7% and 40.1% was observed in the maximum length of axons (sum of both sides) and in the area of axons, respectively, comparing with the SCs + DRG group. Therefore, the BDNF-rich culture medium produces an additional increase in the growth rate of axons, so they can grow faster. In addition, an increase of 27.6%, 30.0% and 40.6% was observed for  $S_{\text{centre}}$ ,  $S_{\text{edge}}$  and  $S_{\text{AUC}}$ , respectively, for the eSCs + DRG group when compared with the SCs + DRG group. This shows an increase of axonal sprouting, so more axons migrate from the DRG body.

Thus, with the eSCs + DRG group we are observing the combined effect of the high alignment of the substrate, the preculture of SCs and the continuous release of BDNF by these cells that increases neuronal regeneration and protection. Therefore, this group would be the one considered to be used as a device for the regeneration of lesions in the nervous system. Furthermore, it should be noted that thanks to the SCs electrotransfection we are achieving an effective and regular release of large amounts of BDNF during the first 10-15 days after its implantation *in vivo*. This is of great importance since the first days after the injury occurs are the most critical ones in the process of remodelling and regenerating an injury of the nervous system. In addition, thanks to the continuous release of BDNF by SCs, it is possible to have a stable BDNF-rich cell environment, solving the problem of the short half-life and the rapid diffusion of BDNF when it is supplied directly in the lesion and avoiding the use of a continuous infusion pump which could lead to greater wound complications and an increased risk of infection<sup>[78,79]</sup>.

#### 4. Conclusions

We have obtained a SCs electroporation protocol that provides a high level of transfection with low cell death, obtaining a large number of live transfected cells. Thanks to this protocol, SCs have been successfully transfected with a plasmid encoding the BDNF protein, which is necessary for the continued survival and maintained phenotype of neurons, promotes survival of dorsal root ganglion neurons, enhances neurogenesis and promotes nerve healing and axonal growth, improving axonal regeneration. Electroporated SCs have been able to both express higher quantities of BDNF protein and secrete them naturally into the culture medium. This has not been previously reported using electroporation techniques with this type of cells *in vitro*. In addition, the quantity of BDNF secreted by electroporated SCs was very high, multiplying by 100 the level of BDNF secretion of non-electroporated SCs.

The co-culture of DRG with non-electroporated and electroporated SCs revealed that the use of PLA-PPy MF substrates precultured with non-electroporated SCs increases both axonal extension and axonal sprouting, but when electroporated SCs are used, there is an additional increment of them. The preculture of SCs is critical so that the axons that grow from the DRG neurons do not have to wait for the SCs that migrate from the DRG body and can be accompanied by the precultured SCs that are present on the substrate, being able to considerably increase its growth rate. Furthermore, when the precultured SCs that are present on the substrate have been previously electroporated with the plasmid encoding the BDNF protein, they release large additional quantities of BDNF to the culture medium, which helps to obtain an additional increase of axonal growth.

Therefore, our system based on a PLA-PPy highly aligned microfiber substrate pre-seeded with electroporated SCs with an increased BDNF secretion is capable of both guiding and accelerating axonal growth and regeneration. For this, the device can be of application for the treatment of injuries of the nervous system, both central and peripheral. The device can be

used either alone or in combination with other devices such as conduits for an inside nerve guidance. In addition, the electrical conductivity of PLA-PPy microfibers allows the electrical stimulation of the device in future studies.

### Supporting Information

Supporting Information is available from the Wiley Online Library or from the author.

### Author contributions

**Fernando Gisbert Roca:** Methodology, Software, Formal analysis, Investigation, Writing – Original Draft, Visualization. **Franck M. Andre:** Methodology, Writing – Review & Editing, Supervision. **Jorge Más Estellés:** Writing – Review & Editing, Supervision, Funding acquisition. **Manuel Monleón Pradas:** Conceptualization, Writing – Review & Editing, Supervision, Funding acquisition. **Lluís M. Mir:** Methodology, Writing – Review & Editing, Supervision, Funding acquisition. **Cristina Martínez-Ramos:** Conceptualization, Methodology, Writing – Review & Editing, Supervision, Funding acquisition.

### Competing interests

The authors declare no competing interests.

### Acknowledgements

The authors acknowledge financing from the Spanish Government's State Research Agency (AEI) through projects DPI2015-72863-EXP and RTI2018-095872-B-C22/ERDF. FGR acknowledges the scholarship FPU16/01833 and the short stay mobility aid EST18/00524 of the Spanish Ministry of Universities. FGR also acknowledges the hosting at the Vectorology and Anti-cancer Therapies Centre (UMR 8203 CNRS). We thank the Electron Microscopy Service at the UPV, where the FESEM images were obtained.

Received: ((will be filled in by the editorial staff))

Revised: ((will be filled in by the editorial staff))

Published online: ((will be filled in by the editorial staff))

### References

1. E. a Huebner, S. M. Strittmatter, *Results Probl. Cell Differ.* **2009**, 48, 339.
2. K. S. Houschyar *et al.*, *Plast. Surg. Int.* **2016**, 2016, 1.
3. W. Daly, L. Yao, D. Zeugolis, A. Windebank, A. Pandit, *J. R. Soc. Interface* **2012**, 9,



- 202.
4. G. C. W. de Ruiter, M. J. A. Malessy, M. J. Yaszemski, A. J. Windebank, R. J. Spinner, *Neurosurg. Focus* **2009**, *26*, E5.
  5. M. D. Tang-Schomer, *Brain Res.* **2018**, *1678*, 288.
  6. M. D. Sarker, S. Naghieh, A. D. McInnes, D. J. Schreyer, X. Chen, *Prog. Neurobiol.* **2018**, *171*, 125.
  7. I. A. Kim *et al.*, *J. Biosci. Bioeng.* **2006**, *101*, 120.
  8. A. W. English, G. Schwartz, W. Meador, M. J. Sabatier, A. Mulligan, *Dev. Neurobiol.* **2007**, *67*, 158.
  9. M. R. Freeman, *Curr. Opin. Neurobiol.* **2006**, *16*, 119.
  10. E. Pompili *et al.*, *Eur. J. Histochem.* **2020**, *64*.
  11. K. R. Jessen, R. Mirsky, A. C. Lloyd, *Cold Spring Harb. Perspect. Biol.* **2015**, *7*, 1.
  12. J. A. Gomez-Sanchez *et al.*, *J. Neurosci.* **2017**, *37*, 9086.
  13. M. Bradl, H. Lassmann, *Acta Neuropathol.* **2010**, *119*, 37.
  14. D. M. McTigue, R. B. Tripathi, *J. Neurochem.* **2008**, *107*, 1.
  15. N. El Seblani, A. S. Welleford, J. E. Quintero, C. G. van Horne, G. A. Gerhardt, *J. Neurosci. Methods* **2020**, *335*, 108623.
  16. K. R. Jessen, P. Arthur-Farraj, *Glia* **2019**, *67*, 421.
  17. G. Nocera, C. Jacob, *Cell. Mol. Life Sci.* **2020**, *1*, doi:10.1007/s00018-020-03516-9.
  18. A. H. Nagahara, M. H. Tuszynski, *Nat. Rev. Drug Discov.* **2011**, *10*, 209.
  19. C. Zuccato, E. Cattaneo, *Nat. Rev. Neurol.* **2009**, *5*, 311.
  20. D. K. Binder, H. E. Scharfman, *Growth Factors* **2004**, *22*, 123.
  21. K. Hanamura, A. Harada, R. Katoh-Semba, F. Murakami, N. Yamamoto, *Eur. J. Neurosci.* **2004**, *19*, 1485.
  22. T. Lopatina *et al.*, *PLoS One* **2011**, *6*.
  23. P. Lu, L. L. Jones, M. H. Tuszynski, *Exp. Neurol.* **2005**, *191*, 344.

24. R. M. Lindsay, *J. Neurosci.* **1988**, *8*, 2394.
25. S. Liu *et al.*, *Acta Biomater.* **2017**, *60*, 167.
26. S. S. Gill *et al.*, *Nat. Med.* **2003**, *9*, 589.
27. G. J. R. Delcroix, P. C. Schiller, J. P. Benoit, C. N. Montero-Menei, *Biomaterials* **2010**, *31*, 2105.
28. E. M. André, C. Passirani, B. Seijo, A. Sanchez, C. N. Montero-Menei, *Biomaterials* **2016**, *83*, 347.
29. P. Menei, C. Montero-Menei, S. R. Whittemore, R. P. Bunge, M. B. Bunge, *Eur. J. Neurosci.* **1998**, *10*, 607.
30. S. T. Sayers, N. Khan, Y. Ahmed, R. Shahid, T. Khan, *J. Mol. Neurosci.* **1998**, *10*, 143.
31. T. K. Kim, J. H. Eberwine, *Anal. Bioanal. Chem.* **2010**, *397*, 3173.
32. A. Pfeifer, I. M. Verma, *Annu. Rev. Genomics Hum. Genet.* **2001**, *2*, 177.
33. S. Hacein-Bey-Abina *et al.*, *N. Engl. J. Med.* **2002**, *346*, 1185.
34. J. Roesler *et al.*, *Blood* **2002**, *100*, 4381.
35. N. B. Woods *et al.*, *Blood* **2003**, *101*, 1284.
36. S. Hacein-Bey-Abina *et al.*, *N. Engl. J. Med.* **2003**, *348*, 255.
37. C. Rosazza, S. H. Meglic, A. Zumbusch, M.-P. Rols, D. Miklavcic, *Curr. Gene Ther.* **2016**, *16*, 98.
38. M. Aspalter *et al.*, *J. Neurosci. Methods* **2009**, *176*, 96.
39. H. B. Wang, M. E. Mullins, J. M. Cregg, C. W. McCarthy, R. J. Gilbert, *Acta Biomater.* **2010**, *6*, 2970.
40. S. Gnani *et al.*, *Mater. Sci. Eng. C* **2015**, *48*, 620.
41. P. M. Tsimbouri, L. E. McNamara, E. V. Alakpa, M. J. Dalby, L. A. Turner, *Tissue Eng. Second Ed.* **2014**, doi:10.1016/B978-0-12-420145-3.00007-9.
42. H. Amani *et al.*, *Adv. Mater. Interfaces* **2019**, *6*, 1.
43. W. Zhu, F. Masood, J. O'Brien, L. G. Zhang, *Nanomedicine Nanotechnology, Biol.*

- Med.* **2015**, *11*, 693.
44. Y. S. Lee, G. Collins, T. Livingston Arinzeh, *Acta Biomater.* **2011**, *7*, 3877.
  45. A. Markus, T. D. Patel, W. D. Snider, *Curr. Opin. Neurobiol.* **2002**, *12*, 523.
  46. P. Lu, M. H. Tuszynski, *Exp. Neurol.* **2008**, *209*, 313.
  47. M. Lykissas, A. Batistatou, K. Charalabopoulos, A. Beris, *Curr. Neurovasc. Res.* **2007**, *4*, 143.
  48. B. S. Bregman, M. McAtee, H. N. Dai, P. L. Kuhn, *Exp. Neurol.* **1997**, *148*, 475.
  49. F. Gisbert Roca, J. Más Estellés, M. Monleón Pradas, C. Martínez-Ramos, *Int. J. Biol. Macromol.* **2020**, *163*, 1959.
  50. F. Gisbert Roca, A. García-Bernabé, V. Compañ Moreno, C. Martínez-Ramos, M. Monleón Pradas, *Macromol. Mater. Eng.* **2020**, 2000584, doi:10.1002/mame.202000584.
  51. D. E. Henton, P. Gruber, J. Lunt, J. Randall, *Nat. Fibers, Biopolym. Biocomposites* **2005**, *48674*, 527.
  52. J. Lunt, *Polym. Degrad. Stab.* **1998**, *3910*, 145.
  53. Y. Ramot, M. Haim-Zada, A. J. Domb, A. Nyska, *Adv. Drug Deliv. Rev.* **2016**, *107*, 153.
  54. D. da Silva *et al.*, *Chem. Eng. J.* **2018**, *340*, 9.
  55. L. X. Wang, X. G. Li, Y. L. Yang, *React. Funct. Polym.* **2001**, *47*, 125.
  56. J. Y. Lee, C. A. Bashur, A. S. Goldstein, C. E. Schmidt, *Biomaterials* **2009**, *30*, 4325.
  57. A. Esfandiari, *World Appl. Sci. J.* **2008**, *3*, 470.
  58. T. H. Le, Y. Kim, H. Yoon, *Polymers (Basel)*. **2017**, *9*.
  59. M. Mattioli-Belmonte *et al.*, *Mater. Sci. Eng. C* **2005**, *25*, 43.
  60. G. Sabouraud, S. Sadki, N. Brodie, *Chem. Soc. Rev.* **2000**, *29*, 283.
  61. C. Li, H. Bai, G. Shi, *Chem. Soc. Rev.* **2009**, *38*, 2397.
  62. S. Aznar-Cervantes *et al.*, *Bioelectrochemistry* **2012**, *85*, 36.

63. J. F. Zhou *et al.*, *Neural Regen. Res.* **2016**, *11*, 1644.
64. P. M. George *et al.*, *Biomaterials* **2005**, *26*, 3511.
65. C. E. Schmidt, V. R. Shastri, J. P. Vacanti, R. Langer, *Proc. Natl. Acad. Sci. U. S. A.* **1997**, *94*, 8948.
66. J. Huang, Z. Ye, X. Hu, L. Lu, Z. Luo, *Glia* **2010**, *58*, 622.
67. H. T. Nguyen *et al.*, *J. Biomed. Mater. Res. - Part A* **2014**, *102*, 2554.
68. Y. Wang *et al.*, *Chin. Med. J. (Engl.)*. **2011**, *124*, 2361.
69. Y. Zou *et al.*, *ACS Appl. Mater. Interfaces* **2016**, *8*, 12576.
70. Y. Xu, Z. Huang, X. Pu, G. Yin, J. Zhang, *Cell Prolif.* **2019**, *52*, 1.
71. G. T. Christopherson, H. Song, H. Q. Mao, *Biomaterials* **2009**, *30*, 556.
72. M. A. Woodruff, D. W. Hutmacher, *Prog. Polym. Sci.* **2010**, *35*, 1217.
73. C. X. F. Lam, D. W. Hutmacher, J. T. Schantz, M. A. Woodruff, S. H. Teoh, *J. Biomed. Mater. Res. A* **2009**, *90*, 906.
74. A. Liew *et al.*, *Hum. Gene Ther. Methods* **2013**, *24*, 289.
75. L. L. Lesueur, L. M. Mir, F. M. André, *Mol. Ther. - Nucleic Acids* **2016**, *5*, e291.
76. S. C. Harward *et al.*, *Nature* **2016**, *538*, 99.
77. J. Schindelin *et al.*, *Nat. Methods* **2012**, *9*, 676.
78. J. Guan *et al.*, *Biomaterials* **2012**, *33*, 1386.
79. E. Palasz *et al.*, *Int. J. Mol. Sci.* **2020**, *21*.

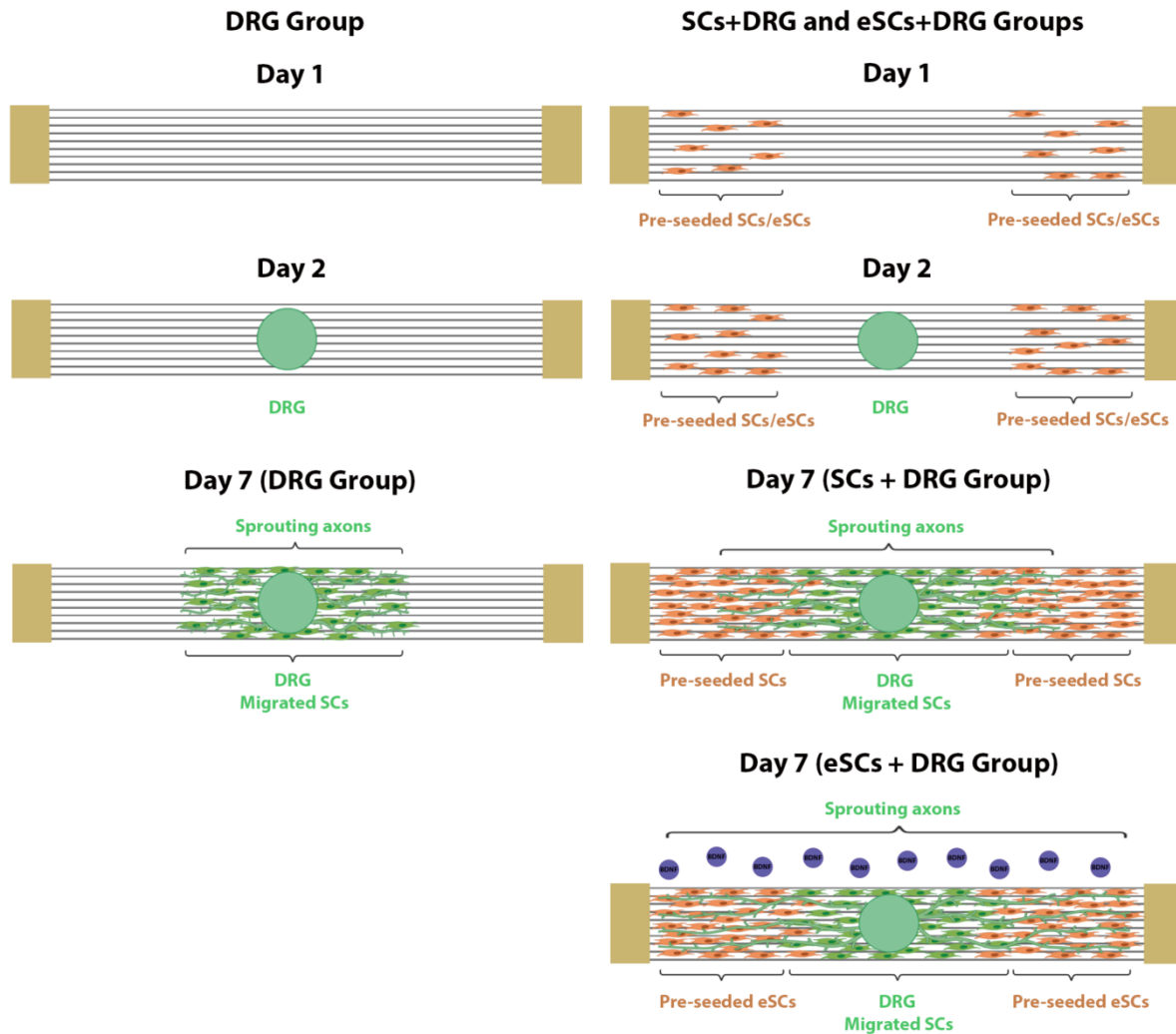


**Figure 1.** Scheme of the different stages of cell culture. First (day 1) the Schwann cells (SCs) and BDNF-SEP transfected Schwann cells (eSCs) are seeded on the substrate extremes for the SCs + DRG and eSCs + DRG groups, respectively. After 24 hours (day 2) one DRG is seeded in the centre of the substrate for all groups. Evaluation is performed after another 5 days of culture (day 7). The neurons present in the DRG body extend their axons over the surface than the SCs covered on the substrate. In the case of the DRG group, the SCs coverage is formed only by SCs that migrated from the DRG body, while in the case of the SC + DRG and eSCs + DRG groups the SCs coverage is made up of both cells that migrated from the DRG body and the pre-seeded Schwann cells (SCs and eSCs, respectively). The presence of pre-seeded SCs is capable of increasing the speed of axonal growth, since the sprouting axons can be accompanied in their growth by the pre-seeded SCs and are not limited by the speed of migration of the SCs originating from the DRG body. Furthermore, in the case of the eSCs + DRG group, the eSCs possess an increased secretion of BDNF that increases even more the axonal growth rate. Created with *BioRender.com*.

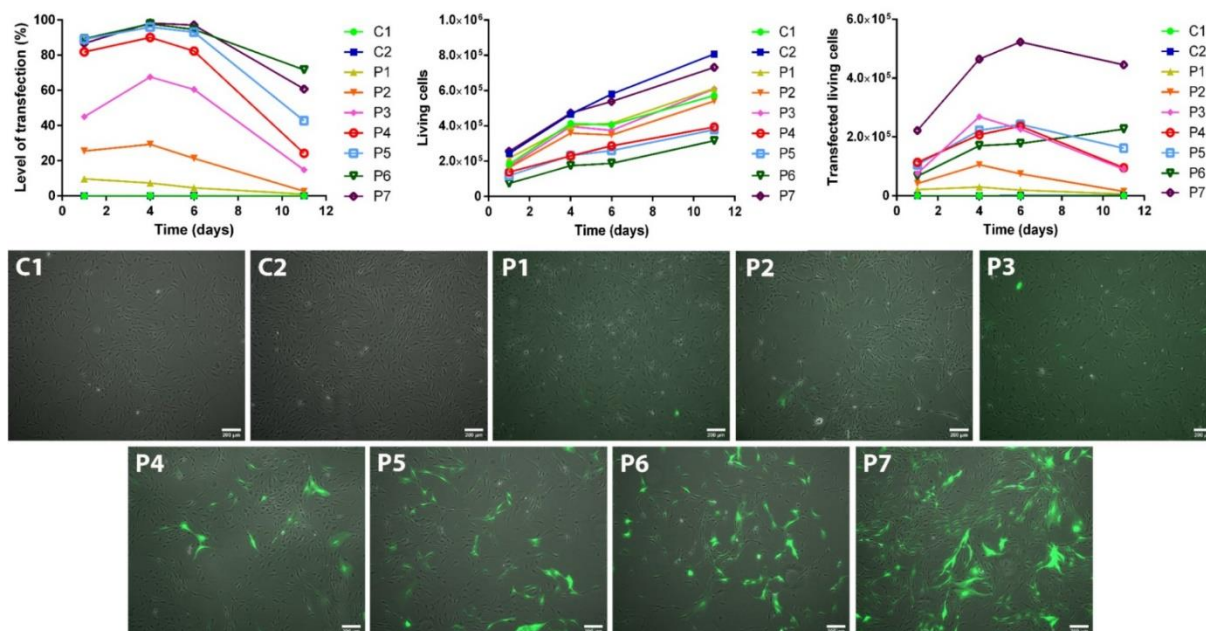


**Figure 2.** Level of transfection, living cells and transfected living cells obtained with the electroporation protocols explained in Table 1. Increasing the quantity of water, the quantity of plasmid and the applied electric field increased the level of transfection but with the cost of a higher cell death. The quantity of transfected living cells was the parameter used to obtain the best balance. To obtain the highest quantity of living cells, a protocol with a high level of transfection (P5) was used but doubling the number of cells (P7). Images of fluorescence microscope after 4 days of cell culture are also included, where can be visually appreciated that the electroporation protocol P7 provides the highest quantity of transfected living cells.

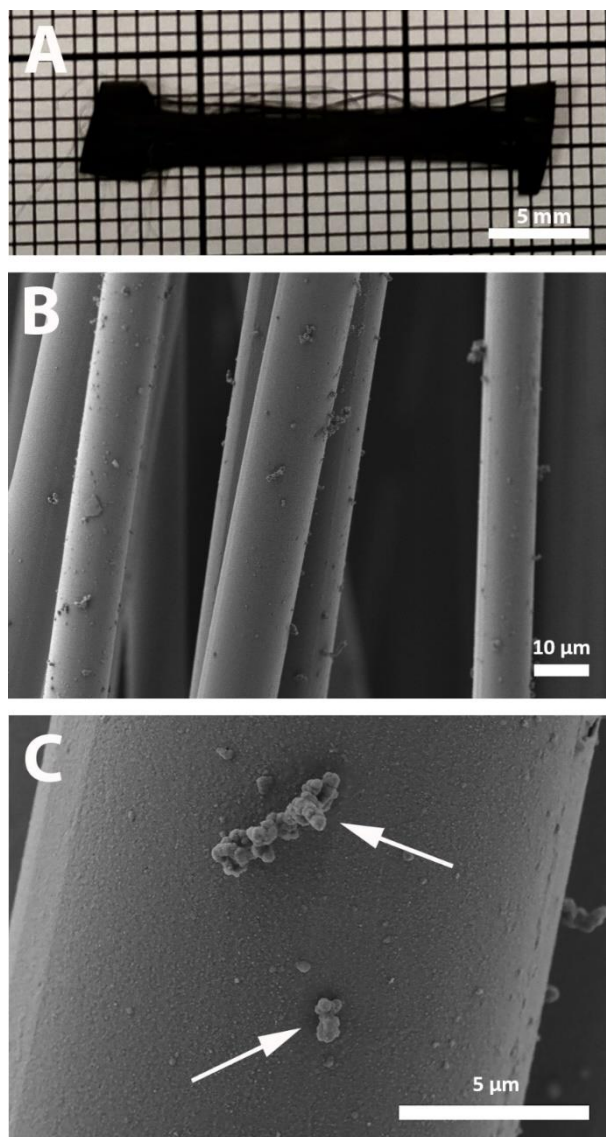


**Figure 3.** Macroscopic (A) and microscopic (B and C) images of PLA-PPy MF substrates used for the co-culture of SCs, eSCs and DRG. PLA MFs (10 μm diameter) were arranged together with a rail shaped form using PCL bands at the extremes that acted as fasteners and coated with PPy via *in situ* polymerization. A homogeneous PPy coating can be observed, forming a fine grain texture. Just some loose aggregates (arrows in C) are present and most of them disappear with repeated washing. Scale bars = 5 mm (A), 10 μm (B) and 5 μm (C).

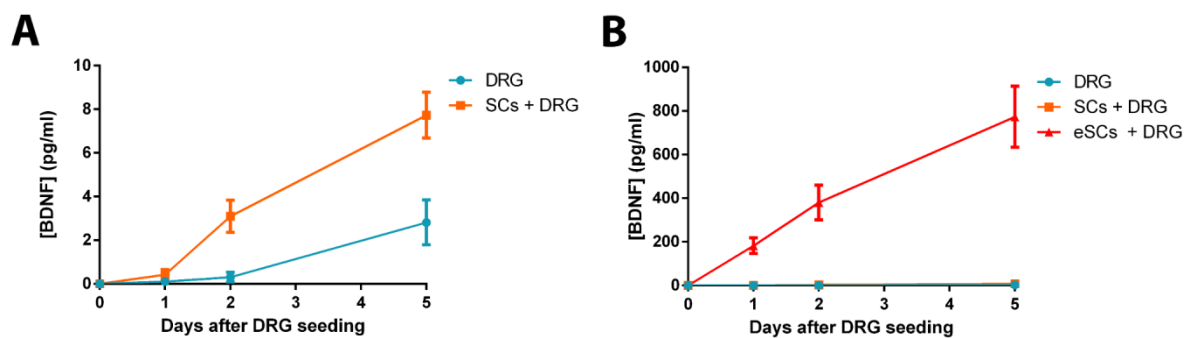


**Figure 4.** A: Magnified detail of B. B: Quantity of BDNF present in the culture medium after 1, 2 and 5 days of cell culture. As can be observed, the BDNF gene transfection of SCs increases a lot the quantity of BDNF protein that is secreted to the culture medium. Values are expressed as mean  $\pm$  SEM.



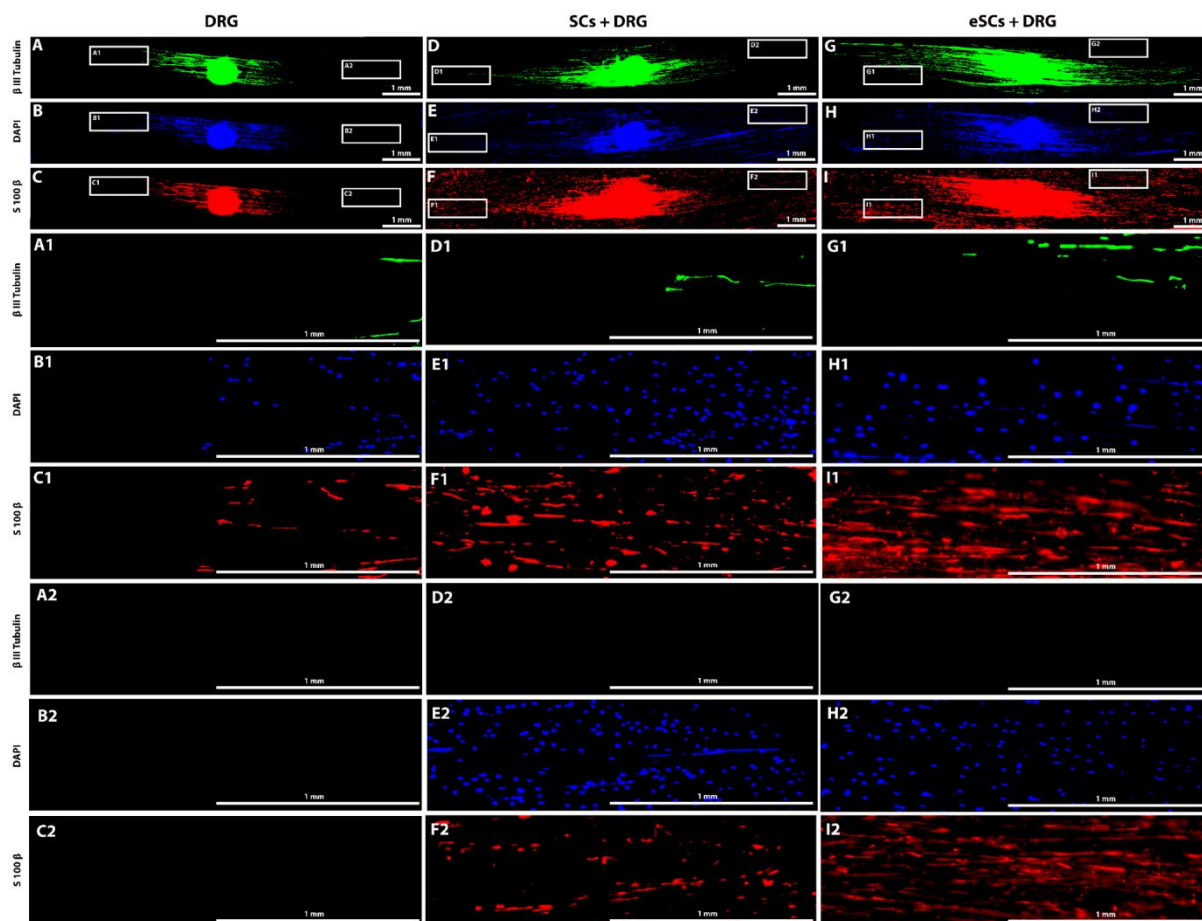


**Figure 5.** Fluorescent microscope images of samples after 5 days of DRG culture. Samples are marked with  $\beta$  III Tubulin to observe the neurons (green colour), DAPI to observe the cell nuclei (blue colour) and S 100  $\beta$  to observe the Schwann cells (red colour). Firstly, a global image of one representative sample is presented for each studied group: DRG (A-C), SCs + DRG (D-F) and eSCs + DRG (G-I). As can be observed, there is a great increment of axonal extension and axonal sprouting when eSCs are used (G) when compared with the sample without SCs (A). For the sample with non-electroporated SCs (D) there is an intermediate behaviour. Therefore, the co-culture of the DRG with non-electroporated SCs increases axonal growth, but the use of eSCs increases this growth even more. The presence of pre-cultured SCs and eSCs is corroborated with image details at two different places of the sample: one at the end of the axons (A1-C1 for the DRG group, D1-F1 for the SCs + DRG group and G1-I1 for the eSCs + DRG group) and another far away from the axons (A2-C2 for the DRG group, D2-F2 for the SCs + DRG group and G2-I2 for the eSCs + DRG group). As can be observed, at the DRG group SCs are only present very near to the axons, indicating that the SCs are migrating from the DRG body along with the axons. However, for SCs + DRG and eSCs + DRG samples, the SCs are present far away from the axons, indicating that those cells are the pre-seeded ones, and not SCs that come from the DRG body. Scale bars = 1 mm.

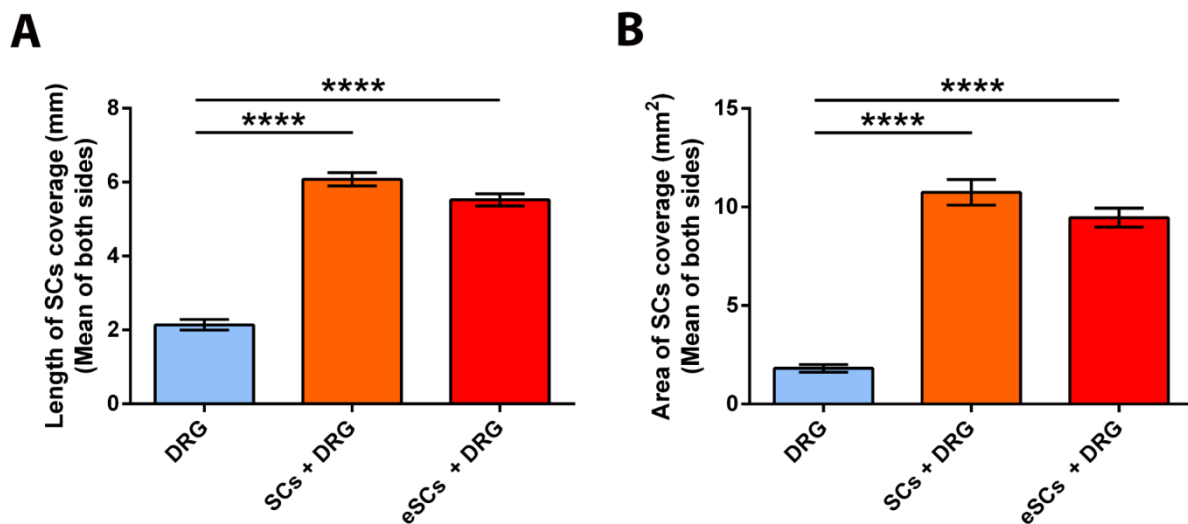


**Figure 6.** Length (A) and area (B) of the SCs coverage present on the substrate after 5 days of DRG culture. As can be observed, the presence of the pre-seeded SCs and eSCs is confirmed by the greater length and area covered by SCs on the substrate for the SCs + DRG and eSCs + DRG groups, respectively. Values are expressed as mean  $\pm$  SEM.

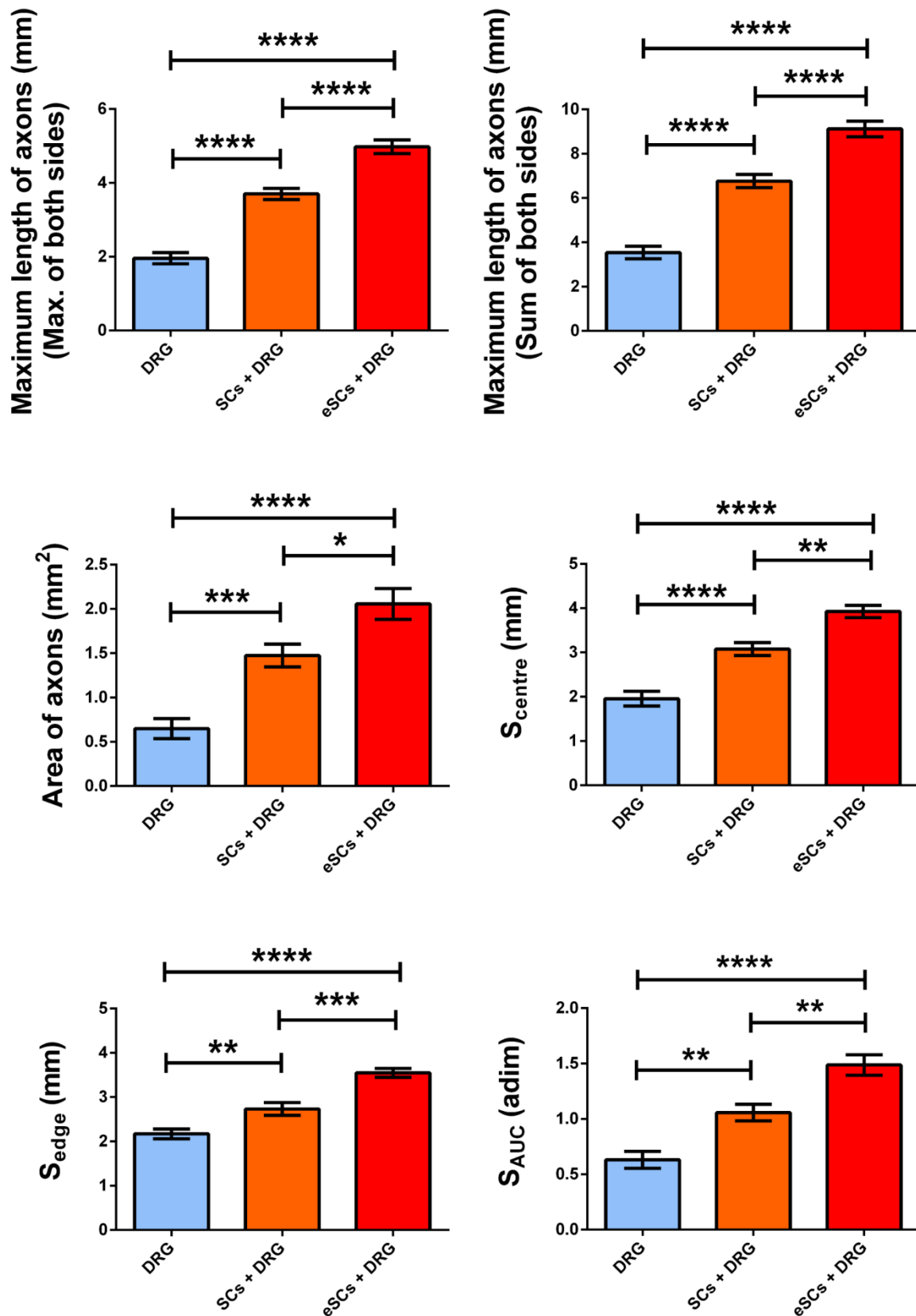


**Figure 7.** Quantification of axonal extension (maximum length of axons and area of axons) and axonal sprouting ( $S_{\text{centre}}$ ,  $S_{\text{edge}}$  and  $S_{\text{AUC}}$ ) after 5 days of DRG culture. The higher values of BDNF protein secreted by eSCs to the culture medium enhanced both axonal extension and axonal sprouting. Values are expressed as mean  $\pm$  SEM.

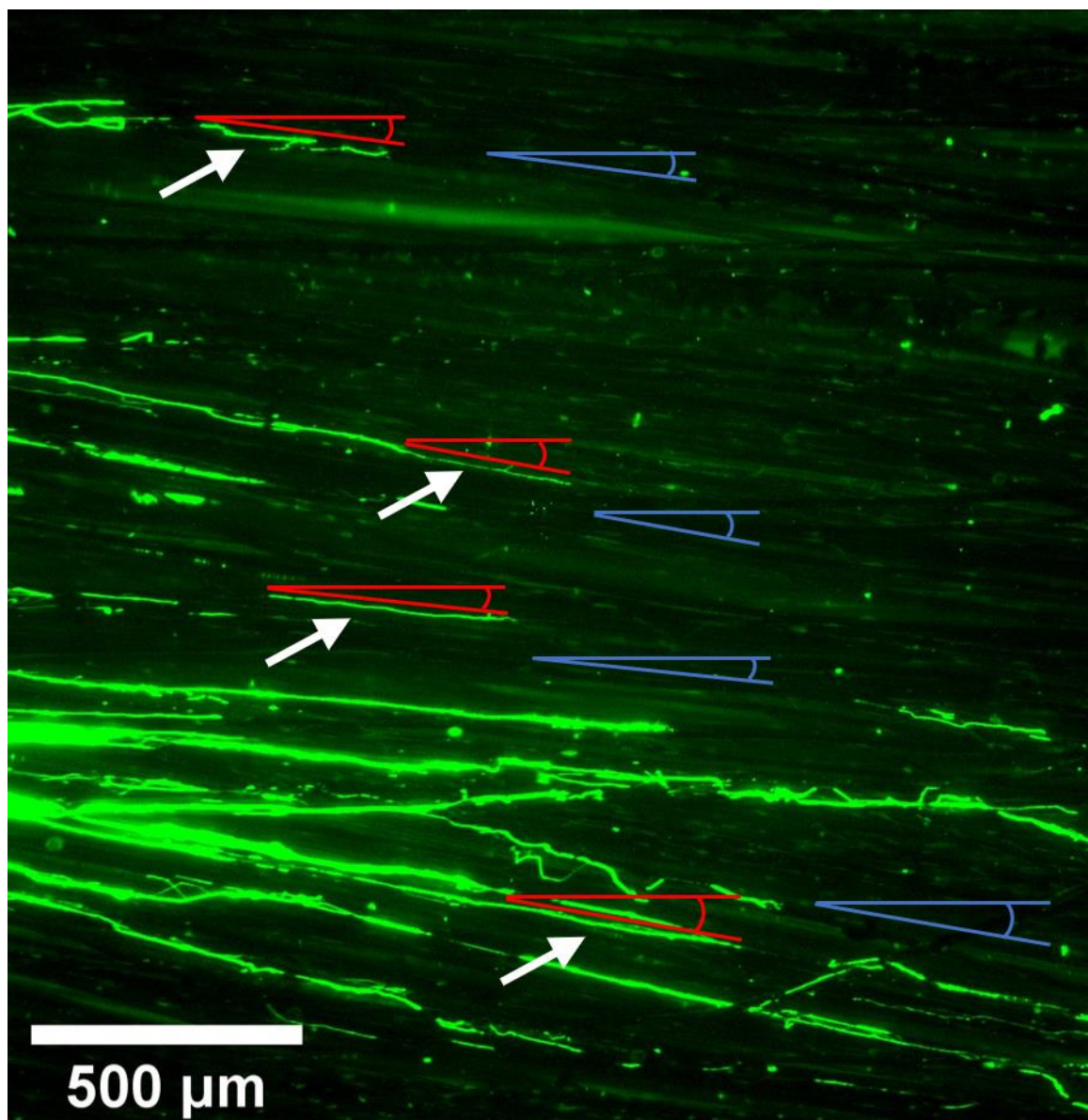


**Figure S1.** Image showing in detail the process followed to measure the angular difference between the direction of axon bundles and the direction of PLA-PPy microfibers. The angle of selected axon bundles (white arrows) is displayed in red colour, while the angle of near PLA-PPy microfibers is displayed in blue colour.

A new biomaterial platform that can be of interest for the treatment of injuries of the nervous system is developed. It combines the use of a substrate based on highly aligned microfibers that guide the axonal growth with the use of gene-transfected Schwann cells with an increased secretion of the brain-derived neurotrophic factor (BDNF) protein that accelerates axonal growth.

Fernando Gisbert Roca, Franck M. André, Jorge Más Estellés, Manuel Monleón Pradas, Lluís M. Mir and Cristina Martínez-Ramos\*

### **BDNF-gene transfected Schwann cells-assisted axonal extension and sprouting on new PLA-PPy microfiber substrates**

ToC figure

